

T h e P h a n t o m L a b o r a t o r y

## C a t p h a n ® 500 and 600 Product Guide

Copyright © 2021

### WARRANTY

THE PHANTOM LABORATORY INCORPORATED (“Seller”) warrants that this product shall remain in good working order and free of all material defects for a period of one (1) year following the date of purchase. If, prior to the expiration of the one (1) year warranty period, the product becomes defective, Buyer shall return the product to the Seller at:

By Truck

The Phantom Laboratory, Incorporated  
2727 State Route 29  
Greenwich, NY12834

By Mail

The Phantom Laboratory, Incorporated  
PO Box 511  
Salem, NY 12865-0511

Seller shall, at Seller’s sole option, repair or replace the defective product. The Warranty does not cover damage to the product resulting from accident or misuse.

IF THE PRODUCT IS NOT IN GOOD WORKING ORDER AS WARRANTED, THE SOLE AND EXCLUSIVE REMEDY SHALL BE REPAIR OR REPLACEMENT, AT SELLER’S OPTION. IN NO EVENT SHALL SELLER BE LIABLE FOR ANY DAMAGES IN EXCESS OF THE PURCHASE PRICE OF THE PRODUCT. THIS LIMITATION APPLIES TO DAMAGES OF ANY KIND, INCLUDING, BUT NOT LIMITED TO, DIRECT OR INDIRECT DAMAGES, LOST PROFITS, OR OTHER SPECIAL, INCIDENTAL, OR CONSEQUENTIAL DAMAGES, WHETHER FOR BREACH OF CONTRACT, TORT OR OTHERWISE, OR WHETHER ARISING OUT OF THE USE OF OR INABILITY TO USE THE PRODUCT. ALL OTHER EXPRESS OR IMPLIED WARRANTIES, INCLUDING, BUT NOT LIMITED TO, THE IMPLIED WARRANTY OF MERCHANT ABILITY AND FITNESS FOR PARTICULAR PURPOSE, ARE HEREBY DISCLAIMED.

### WARNING

This product has an FH3-4 mm/min flame rating and is considered to be flammable. It is advised not to expose this product to open flame or high temperature (over 125° Celsius or 250° Fahrenheit) heating elements.

CTP500  
CTP600

6/October/2021

Product: Catphan®

Model: CTP500 and CTP600

Classification:

Class 1 Medical device in compliance with FDA Medical Device requirements, EU Medical Device Regulation (MDR) 2017/745, and ISO 13485:2016



Designed and Manufactured by:

The Phantom Laboratory

2727 State Route 29

Greenwich, NY 12834 USA

EU Representative:

Raförninn ehf

Suðurhíð 35

IS-105 Reykjavík ICELAND

CTP500



(01)00812266030024

CTP600



(01)00812266030031

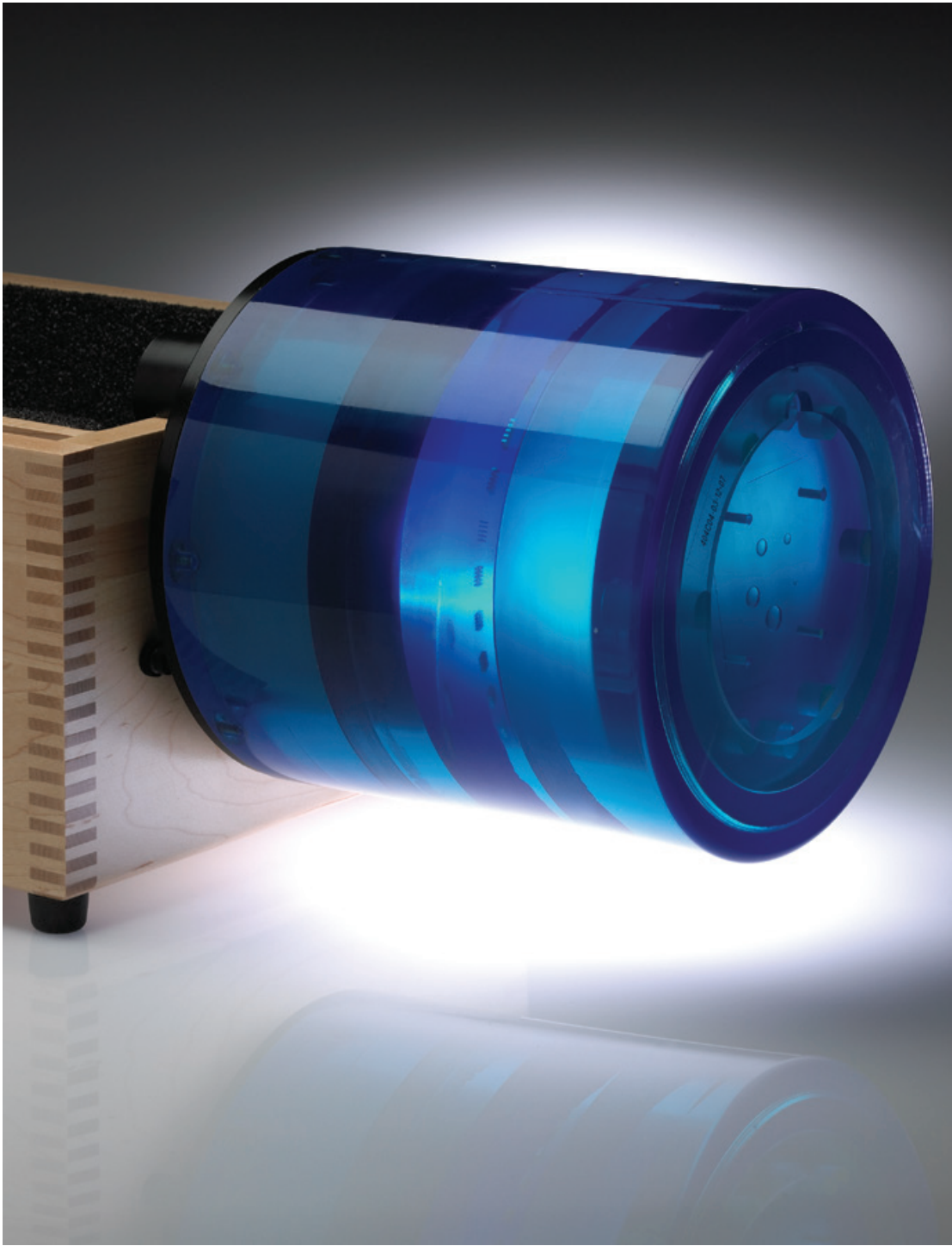


# T h e P h a n t o m L a b o r a t o r y

## **Catphan® Manual**

### *Contents*

Warranty	1
Introduction	5
Multi-Slice CT by David Goodenough, Ph.D.	6
Initial phantom positioning	8
Illustration of Catphan® models	9
Incremental phantom modules positioning	10
Phantom position verification	11
CTP401 and CTP404 modules	12
Patient alignment system check	13
Scan slice geometry (slice width)	14
Scan incrementation	15
Circular symmetry	16
Spatial linearity of pixel size verification	16
Spherical acrylic contrast targets	16
CT or Hounsfield Numbers by David Goodenough, Ph.D.	17
Sensitometry (CT number linearity)	18
CTP591 Bead Geometry Module	19
Measuring slice thickness with a profile made from bead image	21
Additional methods for estimating and measuring slice thickness with bead ramps	22
CTP528 High resolution module with 21 line pair per cm gauge and point source	23
Bead point source for point spread function and MTF	23
Use of automated scanner MTF programs	24
Bead point source (slice sensitivity profile)	26
21 Line pair per centimeter high resolution gauge	27
CTP515 Low contrast module with supra-slice and subslice contrast targets	28
CTP486 Image uniformity module	30
Installation and removal of test modules	31
Optional phantom annuli	32
CTP541 16cm housing	33
Smári analysis service	34
Bibliography	35



## **Introduction**

The Phantom Laboratory and physicist, David J. Goodenough, Ph.D., are continually developing and researching new tests and modifications for the Catphan® phantoms. The test objects that make up the current Catphan® models embody more than a quarter century of scientific evaluation and field experience. This manual outlines the applications of each module contained in the Catphan® 500 and 600 phantoms.

We do not make specific recommendations on the content of your quality assurance program, because each medical imaging facility has its own unique set of requirements. A sample program is provided to give you ideas for possible program content. We suggest a review of local governing regulations, manufacturers' specifications and the needs of your radiologists and physicists before developing your CT quality assurance program.

The Catphan® instructional video, which illustrates the phantom setup and scanning of the different Catphan® sections, is also available.

If you have any additional questions please contact The Phantom Laboratory at:

Phone: 800-525-1190 or 518-692-1190

Fax: 518-692-3329

email: [sales@phantomlab.com](mailto:sales@phantomlab.com)

Additional product information is available at: [www.phantomlab.com](http://www.phantomlab.com)

## **Multi-Slice CT**

**by David J. Goodenough, Ph.D.**

At the request of The Phantom Laboratory I have put together this summary for physicists who are familiar with CT image performance measurements and have not had experience with multi-slice CT scanners.

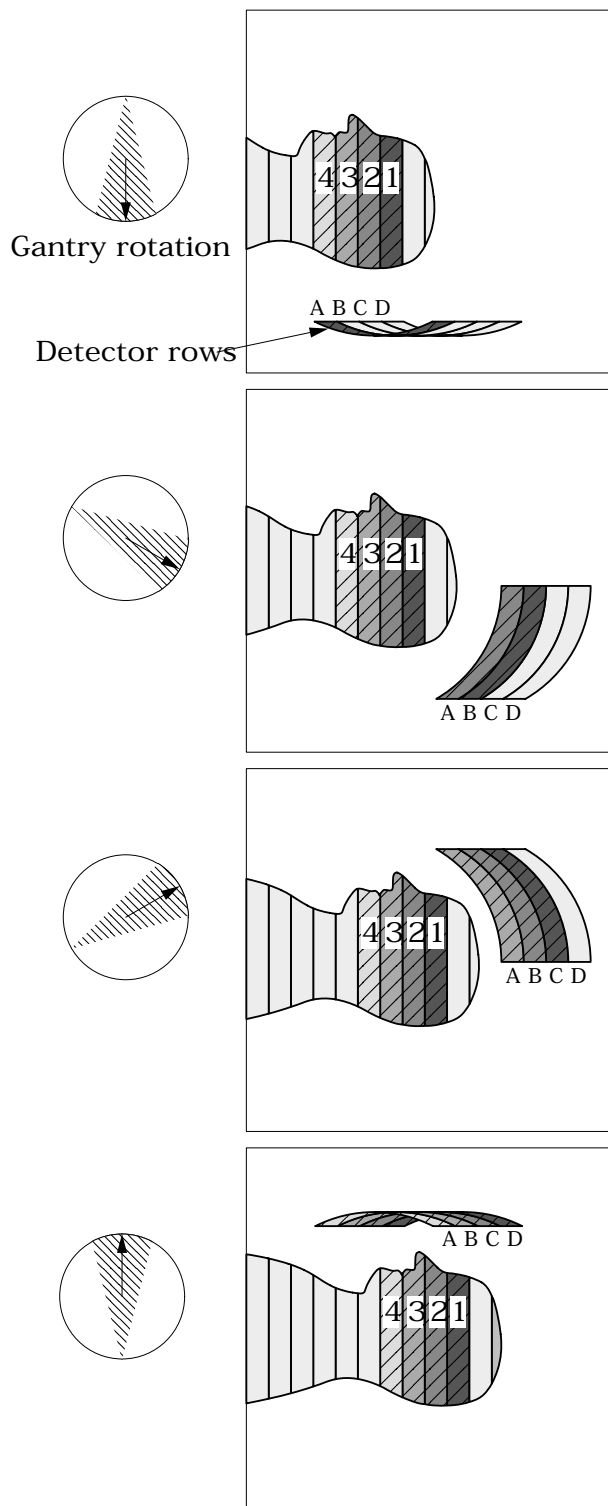
Multi-slice uses the same basic approach to image reconstruction as axial single slice CT. Both modalities use the data from the detectors (positioned 360° around the patient) to reconstruct the axial patient images. The key difference between axial single slice CT and multi-slice is the axial image produced by single slice CT is developed from a single row of detectors, and the axial image made from a multi-slice scanner uses segments from several rows of detectors. With a multi-slice scan, as the patient moves through the gantry and the tube rotates around the patient, the detector rows utilized change as the patient and gantry move (see sketch on the next page).

Additional variables in reconstruction result as the patient slice moves from one row of detectors to the next and the scanner reconstructs the images based on weighted averages between the relevant rows. In this way, multi-slice CT is analogous to spiral or helical single slice CT, but where the reconstruction is obtained from the combined slices rather than the interpolation between the readings of a single moving slice. Now add in focal spot variables and a little scatter to define in more detail the challenges and variables included in the reconstruction of a multi-slice image.

Because in spiral mode each multi-slice image is reconstructed from an ensemble of data taken in different positions across the beam and from different detector rows, the overall image quality differences between images are minimal. In the spiral mode each slice represents data as seen from all detector rows in a sense a kind of averaging of detector row positions. However, if you use a multi-slice “step and shoot” mode, where each of the slices may be created from a single detector row (or rows depending on the selected slice thickness) with a consistent collimation, the differences between the slices will be evident. Step and shoot mode in a multi-slice CT scanner is operated like a conventional axial scanner by imaging with a fixed table position and then moving the table to the next position before imaging the next section of the phantom with a fixed table position. For example, with a step and shoot 8 slice scan it is expected that the middle slice numbers 4 and 5 will have better uniformity than outer slice numbers 1 and 8 because of the scanner x-ray beam geometry. However, if 1 and 8 or 4 and 5 are not similar, this may indicate a problem with the scanner.

When assessing a scanner with a step and shoot mode, it is important to cover the full detector width with the selected test objects. If the test object is narrower than the slice, the table will need to be incremented between scanning sequences so the object can be scanned by all active rows of the detector.

I recommend scanning through the entire phantom using different multi-slice spiral protocols for performance evaluations, as well as using the step and shoot approach for the bead ramps where slice geometry and the MTF can be measured for each slice and uniformity section where the signal to noise and uniformity of each slice (detector row) can be evaluated.



This simplified illustration of a multi-slice sequence shows how the slices are reconstructed with information for different detector rows. The imaging sequence of the first selected slice (slice 1) of the patient begins when slice 1 moves over detector row A. As the tube continues to rotate and the patient continues to move through the gantry, slice 1 is picked up by the detectors in row B. At the same time slice 2, which was outside the detector view, is picked up by the detectors in row A. This sequence continues until the last selected region of the patient has passed through all the active detector rows.

The Catphan® phantom is positioned in the CT scanner by mounting it on the case.

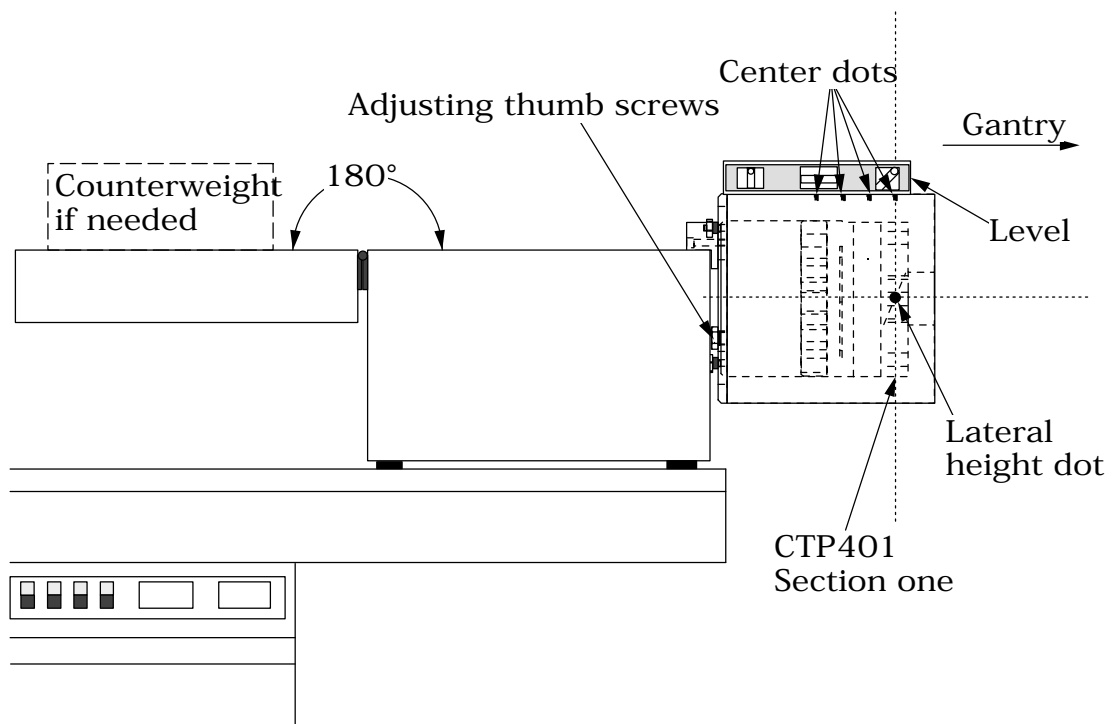
Place the phantom case on the gantry end of the table with the box hinges away from the gantry. It is best to place the box directly on the table and not on the table pads.

Open the box, rotating the lid back 180°. If you are using an annulus, additional weight will need to be placed in the box to counterweigh the phantom. The patient straps can be used for additional stability.

Remove the phantom from the box and hang the Catphan® from the gantry end of the box. Make sure the box is stable with the weight of the phantom and is adequately counterweighed to prevent tipping.

Use the level and adjusting thumb screws to level the Catphan®. Once the phantom is level, slide the phantom along the end of the box to align the section center dots on the top of the phantom with the x axis alignment light.

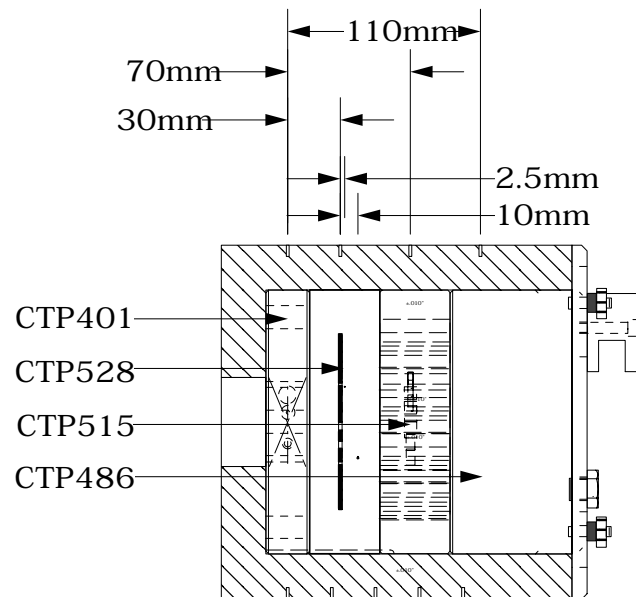
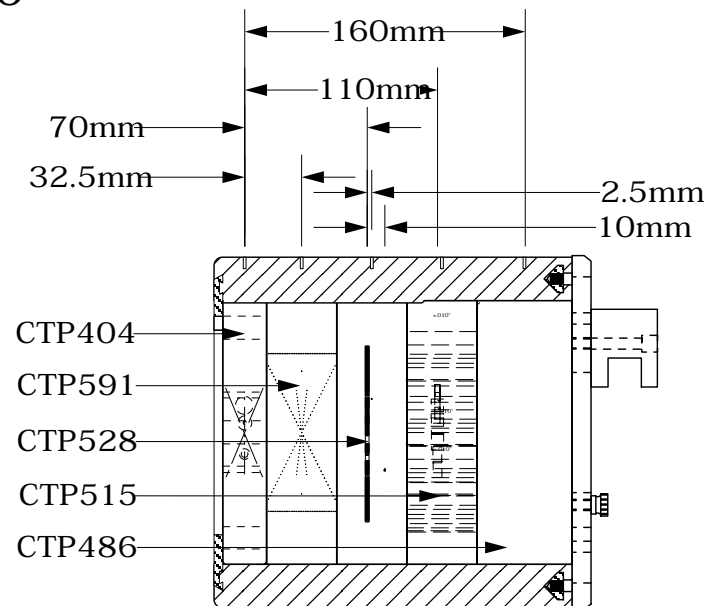
Use the table height and indexing drives to center the first section's (CTP401 or CTP404, Slice Geometry) alignment dots on the side and top of the phantom with the scanner alignment lights.



The z axis scan alignment position can be selected from the localizer scan, by centering the slice at the intersection of the crossed wire image created by the slice width ramps.

Scan the first section (CTP401 or CTP404) and check the image for proper alignment as illustrated in the **Phantom position verification** section.



**Illustration of Catphan® 500 and 600 models****Catphan® 500****Catphan® 600**

### Incremental phantom module positioning

The Catphan® phantoms are designed so all test sections can be located by precisely indexing the table from the center of section 1 (CTP401 or CTP404) to the center of each subsequent test module. This design eliminates the need to remount the phantom once the position of section 1 (CTP401 or CTP404) has been verified. The indexing distances from section 1 are listed below. Additional illustrations on the preceding page show the test modules and their index spacing. Phantom position and alignment verification is described on the next page.

Catphan® 500 test module locations:

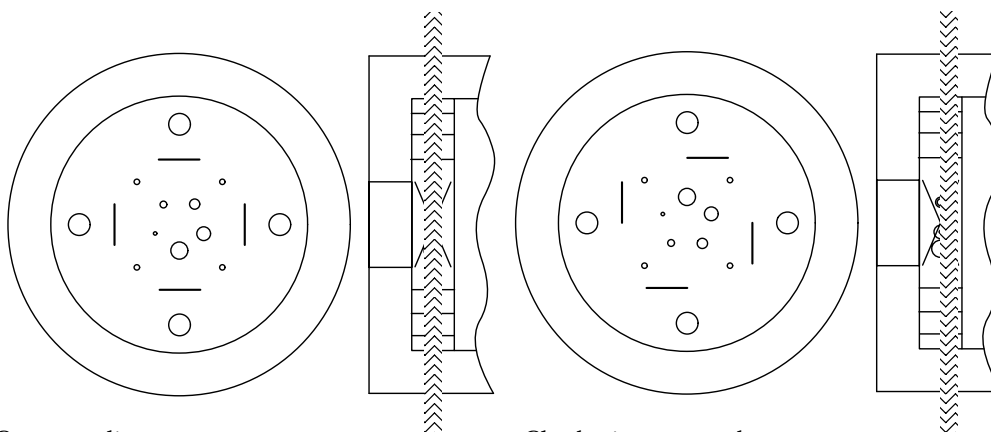
Module	Distance from CTP401 center
CTP528, 21 line pair high resolution	30mm
CTP528. Point source	40mm
CTP515, Subslice and supra-slice low contrast	70mm
CTP486, Solid image uniformity module	110mm

Catphan® 600 test module locations:

Module	Distance from CTP404 center
CTP591 Bead geometry	32.5mm
CTP528, 21 line pair high resolution	70mm
CTP528. Point source	80mm
CTP515, Subslice and supra-slice low contrast	110mm
CTP486, Solid image uniformity module	150mm

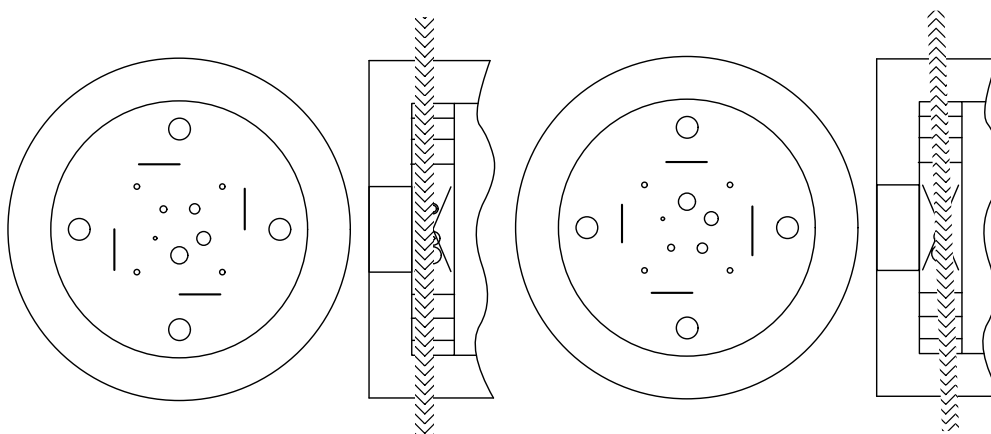
## Phantom position verification

By evaluating the scan image of section 1 (CTP401 or CTP404) the phantom's position and alignment can be verified. The section contains 4 wire ramps which rise at 23° angles from the base to the top of the module. The schematic sketches below indicate how the ramp images change if the scan center is above or below the z axis center of the test module. The use of the scanner's grid image function may assist in evaluation of phantom position.



**Correct alignment**  
In this image the x, y symmetry of the centered ramp images indicates proper phantom alignment.

**Clockwise ramp skew**  
When the ramps are evenly rotated clockwise from center, the phantom is too far into the gantry.



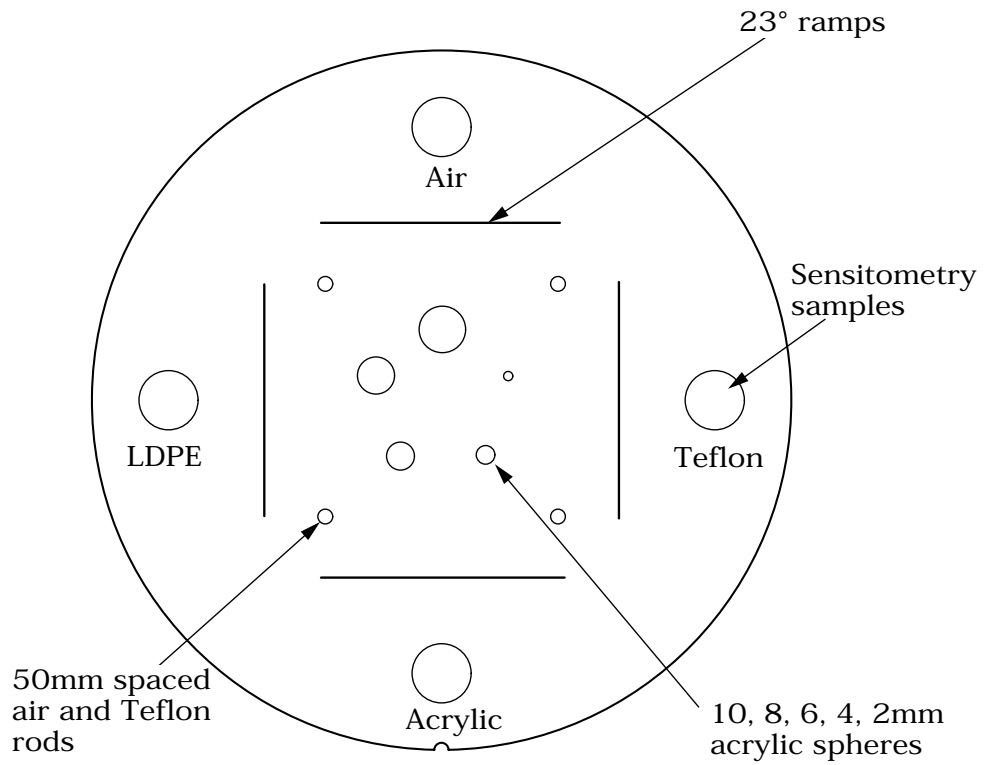
**Counter-clockwise ramp skew**  
When the ramps are evenly rotated counter-clockwise from center, the phantom needs to be moved toward the gantry.

**Non symmetrical ramp images**  
Poor alignment with the z axis is indicated when the ramps are not symmetrical in lengths and rotation.

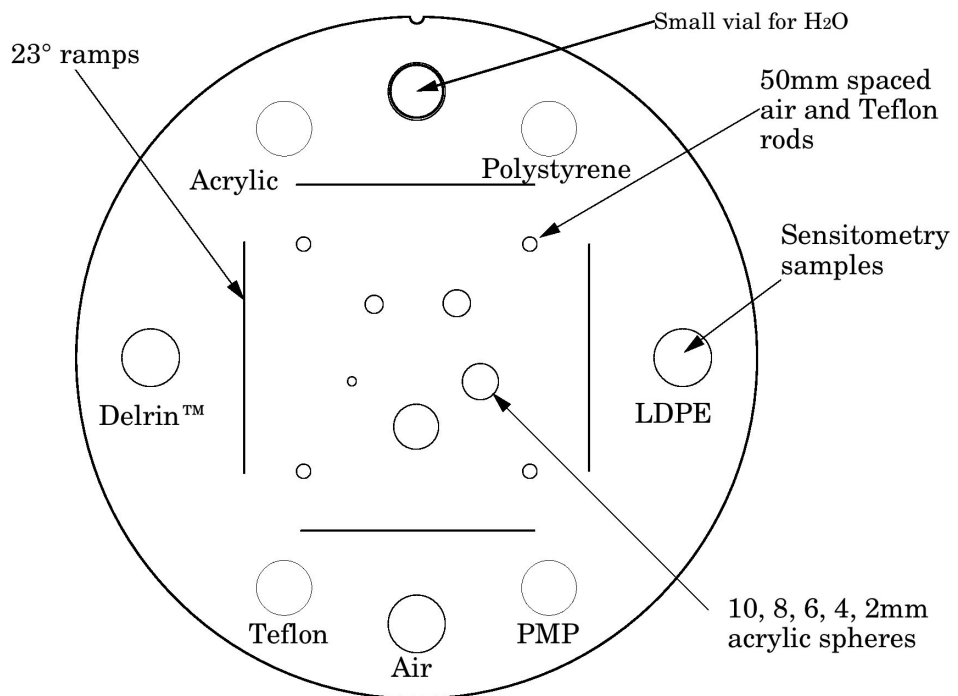
If misalignment is indicated by the scan image, the phantom should be repositioned to obtain proper alignment and then rescanned. If the images of the repositioned phantom duplicate the original misalignment indications, the scanner's alignment lights may require adjustment (contact your local service engineer).

Once correct alignment has been established, you can proceed with the tests.

**CTP401 Module with slice width, sensitometry and pixel size**

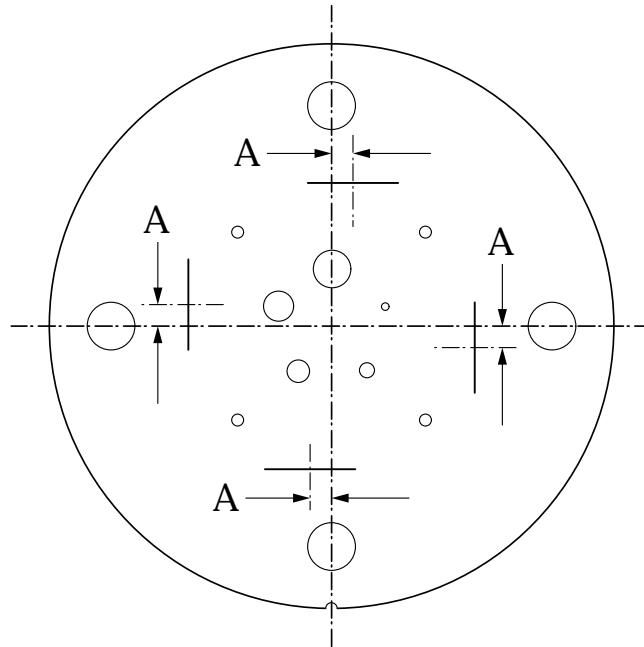


**CTP404 Module with slice width, sensitometry and pixel size**



### Patient alignment system check

The laser, optical, and mechanical patient alignment system can be checked for accuracy. Align the white dots on the phantom housing with the alignment lights as discussed in **Initial phantom positioning**. The scanned image should show good alignment as discussed in **Phantom position verification**.

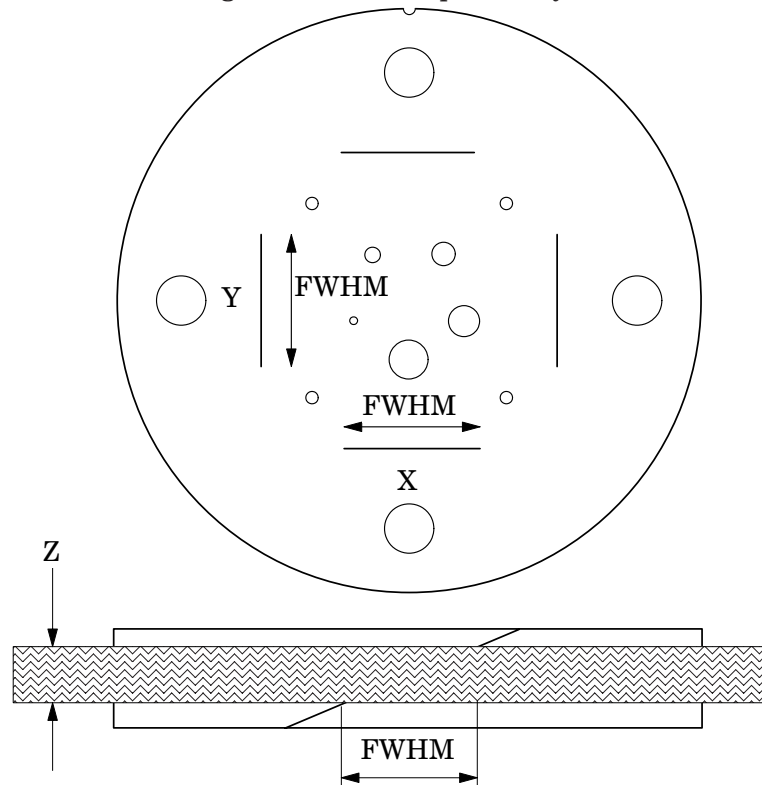


For measuring the z axis alignment accuracy, measure from the center of the ramp image to the part of the ramp which aligns with the center of the phantom and sensitometry samples. Multiply the distance A by 0.42 to determine the z axis alignment light accuracy. To evaluate x and y accuracy, measure from the center of the phantom to the center of the scan field by use of the grid function or knowledge of the central pixel location.

The accuracy of the localizer, pilot or scout view can be checked. To check this function perform a localization scan of the phantom. Align an axial scan at the crossing point of the wire ramps. Scan this axial cut and check the misalignment as discussed above.

### Scan slice geometry (slice width)

Section 1 has two pairs of 23° wire ramps: one pair is oriented parallel to the x axis; the other pair to the y axis. These wire ramps are used to estimate slice width measurements and misalignment errors as previously discussed.



The 23° wire ramp angle is chosen to improve measurement precision through the trigonometric enlargement of 2.38 in the x-y image plane.

To evaluate the slice width (Zmm), measure the Full Width at Half Maximum (FWHM) length of any of the four wire ramps and multiply the length by 0.42:

$$(Z_{mm}) = FWHM * 0.42$$

To find the FWHM of the wire from the scan image, you need to determine the CT number values for the peak of the wire and for the background.

To calculate the CT number value for the maximum of the wire, close down the CT “window” opening to 1 or the minimum setting. Move the CT scanner “level” to the point where the ramp image just totally disappears. The CT number of the level at this position is your peak or maximum value.

To calculate the value for the background, use the region of interest function to identify the “mean” CT number value of the area adjacent to the ramp.

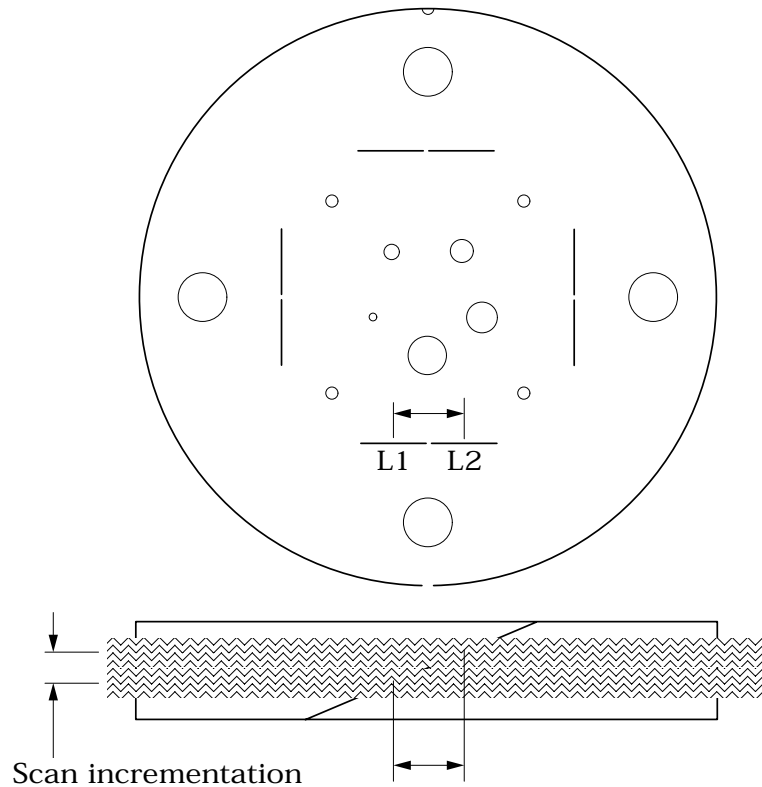
Using the above CT values, determine the half maximum:

First calculate the net peak... (CT # peak - background = net peak CT #)

Calculate the 50% net peak... (net peak CT # ÷ 2 = 50% net peak CT #)

Calculate the half maximum CT number...  
(50% net peak CT # + background CT # = half maximum CT #)

Now that you have determined the half maximum CTnumber, you can measure the full width at half maximum of the ramp. Set the CT scanner level at the half maximum CT value and set your window width at 1. Measure the length of the wire image to determine the FWHM. Multiply the FWHM by 0.42 to determine the slice width.



Schematic illustration of two sequential 5mm scans superimposed. L1 is the center point on the 23° ramp in the first scan image and L2 is the center point on the 23° ramp on the second image.

### Scan incrementation

Use the wire ramps to test for proper scanner incrementation between slices, and for table movement.

Scan section 1 using a given slice width, (e.g. 5mm). Increment the table one slice width (e.g. 5mm) and make a second scan. Establish the x and y coordinates for the center of each ramp image. Calculate the distance between these points and multiply by the 23° ramp angle correction factor of 0.42.

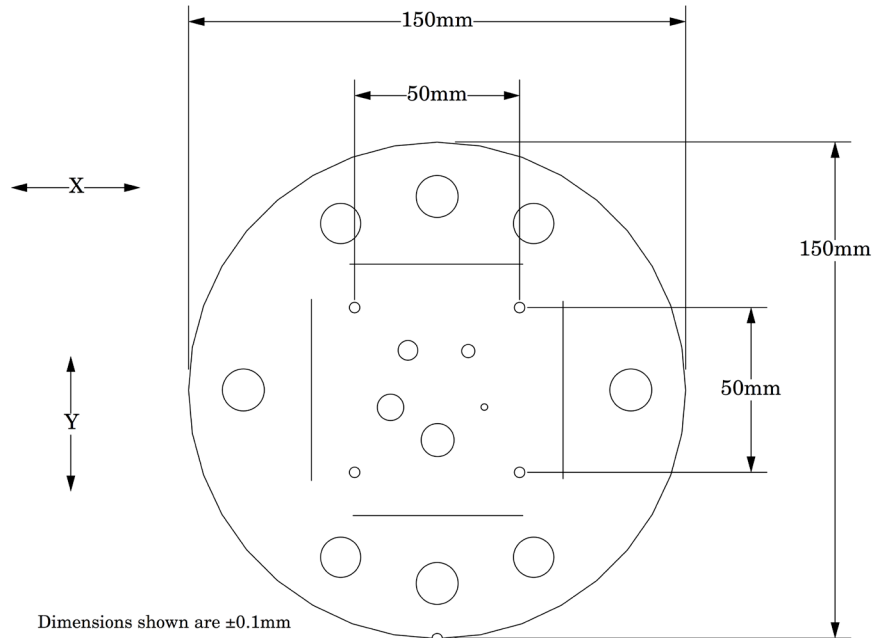
$$0.42(L1 - L2) = \text{scan incrementation}$$

This test can also be used to test table increment accuracy. Scan the section and increment the table 30mm in and out of the gantry and scan again. The ramp centers should be the same on both images.

$$0.42(L1 - L2) = 0$$

### Circular symmetry of display system

The circular phantom sections are used to test for circular symmetry of the CT image, including calibration of the CT display system. If an elliptical image is produced, the x-y balance of the image display system should be adjusted.



Measuring spatial linearity in x and y axes.

### Spatial linearity of pixel size verification

This section has four holes (one with a Teflon pin). These 3mm diameter holes are positioned 50mm on center apart. By measuring from center to center the spatial linearity of the CT scanner can be verified. Another use is to count the number of pixels between the hole centers, and by knowing the distance (50mm) and number of pixels, the pixel size can be verified.

The Teflon pin is used for identification and orientation only. The ability to change the Teflon pin position enables organizations with more than one Catphan® phantom to identify their phantoms by images of the first section.

### Spherical acrylic contrast targets

The section has five acrylic spheres located in a 30mm diameter circular pattern. These spheres are used to evaluate the scanner's ability to image volume averaged spheres. The sphere diameters are 2, 4, 6, 8, and 10mm.



## CT or Hounsfield Numbers by David Goodenough, Ph.D.

Users of CT systems are often surprised when the CT number of a given tissue or substance is different from what they expect from previous experience. These differences do not usually indicate problems of a given CT scanner, but more likely arise from the fact that CT numbers are not universal. They vary depending on the particular energy, filtration, object size and calibration schemes used in a given scanner. One of the problems is that we are all taught that the CT number is given by the equation:

$$CT\# = k(\mu - \mu_w)/\mu_w,$$

where  $k$  is the weighting constant (1000 is for Hounsfield Scale),  $\mu$  is the linear attenuation coefficient of the substance of interest, and  $\mu_w$  is the linear attenuation coefficient of water. Close review of the physics reveals that although the above equation is true to first order, it is not totally correct for a practical CT scanner. In practice,  $\mu$  and  $\mu_w$  are functions of energy, typical x-ray spectra are not monoenergetic but polychromatic, and a given spectrum emitted by the tube is “hardened” as it is transmitted (passes) through filter(s) and the object, finally reaching the detector. More accurately,  $\mu = \mu(E)$ , a function of energy. Therefore:

$$CT\#(E) = k(\mu(E) - \mu_w(E))/\mu_w(E)$$

Because the spectrum is polychromatic we can at best assign some “effective energy”  $\hat{E}$  to the beam (typically some 50% to 60% of the peak kV or kVp). Additionally, the CT detector will have some energy dependence, and the scatter contribution (dependent on beam width and scanned object size, shape, and composition) may further complicate matters. Although the CT scanner has a built in calibration scheme that tries to correct for beam hardening and other factors, this is based on models and calibration phantoms that are usually round and uniformly filled with water, and will not generally match the body “habitus” (size, shape, etc.).

The situation is really so complicated that it is remarkable that tissue CT numbers are in some first order ways “portable”!

In light of the above we can examine a parameter of CT performance, the “linearity scale”, as required by the FDA for CT manufacturer’s performance specifications.

The linearity scale is the best fit relationship between the CT numbers and the corresponding  $\mu$  values at the effective energy  $\hat{E}$  of the x-ray beam.

The effective energy  $\hat{E}$  is determined by minimizing the residuals in a best-fit straight line relationship between CT numbers and the corresponding  $\mu$  values.

In review, we will encounter considerable inter and intra scanner CT number variability. CT numbers can easily vary by 10 or more based on kVp, slice thickness, and object size, shape, and composition. There is some possibility of the use of iterative techniques and/or dual energy approaches that might lessen these effects, but certainly CT numbers are not strictly portable and vary according to the factors listed above.

More complete scientific references are contained in the bibliography. In particular, references 2, 13, 14, and 20 are recommended for those with greater interest in the topic.

### Sensitometry (CT number linearity)

The CTP404 module has sensitometry targets made from Teflon®, Delrin®, acrylic, Polystyrene and low density polyethylene (LDPE), polymethylpentene (PMP) and air. The Catphan® 600 is also equipped with a small vial which can be filled with water and inserted into the top hole of the CTP404 module. The CTP401 module has Teflon, acrylic and low density polyethylene (LDPE) and air targets. These targets range from approximately +1000 H to -1000 H.

The monitoring of sensitometry target values over time can provide valuable information, indicating changes in scanner performance.

#### Nominal material formulation and specific gravity

Material	Formula	Z <sub>eff</sub> <sup>1</sup>	Specific Gravity <sup>2</sup>	HU range <sup>3</sup>
Air	.78N, .21O, .01Ar	8.00	0.00	-1046 : -986
PMP	[C <sub>6</sub> H <sub>12</sub> (CH <sub>2</sub> )]	5.44	0.83	-220 : -172
LDPE	[C <sub>2</sub> H <sub>4</sub> ]	5.44	0.92	-121 : -87
Water	[H <sub>2</sub> O]	7.42	1.00	-7 : 7
Polystyrene	[C <sub>8</sub> H <sub>8</sub> ]	5.70	1.03	-65 : -29
Acrylic	[C <sub>5</sub> H <sub>8</sub> O <sub>2</sub> ]	6.47	1.18	92 : 137
Delrin®	Proprietary	6.95	1.42	344 : 387
Teflon®	[CF <sub>2</sub> ]	8.43	2.16	941 : 1060

#### Electron density and relative electron density

Material	Electron Density (10 <sup>23</sup> e/g)	Electron Density (10 <sup>23</sup> e/cm <sup>3</sup> )	Relative Electron Density <sup>4</sup>
Air	3.002	0.004	0.001
PMP <sup>5</sup>	3.435	2.851	0.853
LDPE <sup>6</sup>	3.435	3.160	0.945
Water	3.343	3.343	1.000
Polystyrene	3.238	3.335	0.998
Acrylic	3.248	3.833	1.147
Delrin®	3.209	4.557	1.363
Teflon®	2.890	6.243	1.868

<sup>1</sup> Z<sub>eff</sub>, the effective atomic number, is calculated using a power law approximation.

<sup>2</sup> For standard material sensitometry inserts The Phantom Laboratory purchases a multiple year supply of material from a single batch. Samples of the purchased material are then measured to determine the actual specific gravity. The specific gravity of air is taken to be .0013 at standard temperature and pressure. For custom cast materials the specific gravity of each cast batch is noted and supplied with the phantom.

<sup>3</sup> These are maximum and minimum measured values from a sample of 94 scans using different scanners and protocols. HU can vary dramatically between scanners and imaging protocols and numbers outside of this range are not unusual.

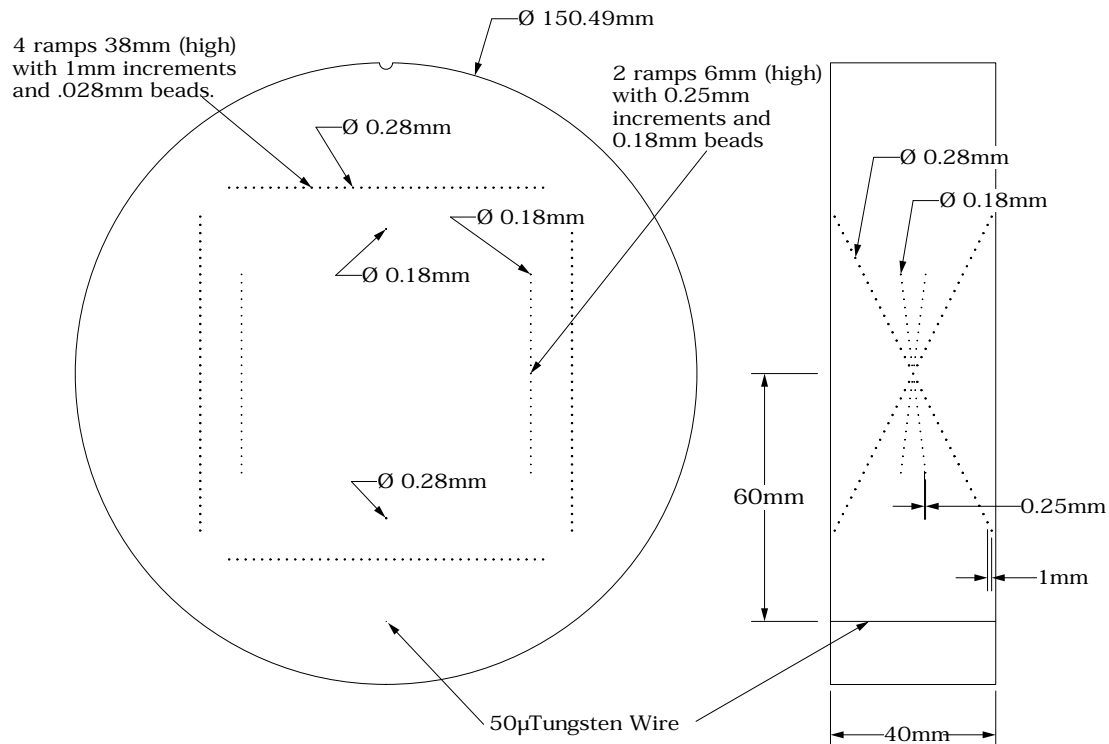
<sup>4</sup> Relative Electron Density is the electron density of the material in e/cm<sup>3</sup> divided by the electron density of water (H<sub>2</sub>O) in e/cm<sup>3</sup>.

<sup>5</sup> Polymethylpentene

<sup>6</sup> Low Density Polyethylene

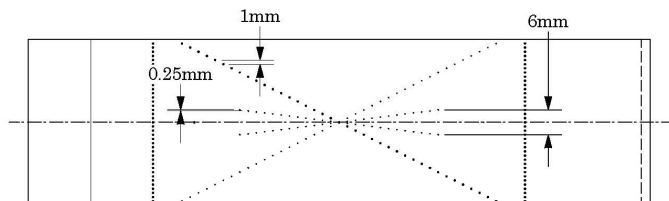
An excel file with the mas attenuation coefficients for the sensitometry materials can be downloaded from our web site.

## CTP591 Bead Geometry Module

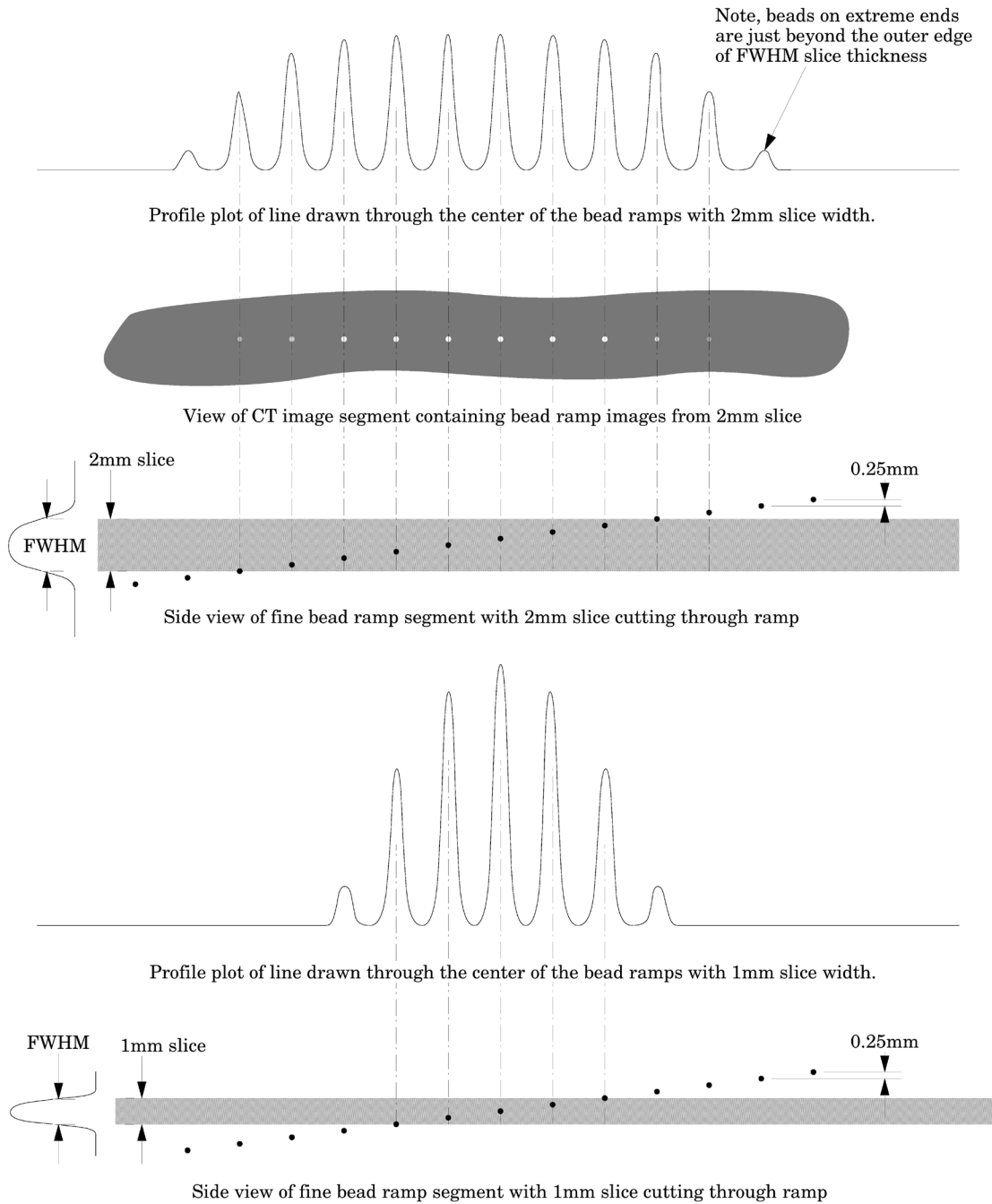


The Bead Geometry Module contains 3 pairs ( 2 coarse and 1 fine) of opposed ramps and 2 individual beads. Two of the ramp pairs have 0.28mm diameter beads, spaced 1mm on center in the z direction. The other ramp pair has 0.18mm diameter beads, spaced 0.25mm on center in the z direction. The 2 individual beads are 0.28mm and 0.18mm in diameter. A  $50\mu$  diameter tungsten wire is located 6cm from the center of the module. The wire and beads create point spreads that can be used to calculate the MTF (see the CTP528 section of this manual).

In the sketch below you can see both the fine and coarse bead ramps. The fine has .25mm y axis steps and the coarse have 1mm steps. You will also see the ramps crossing due to the fact that the ramps are placed in pairs and you see both ramps in the pair from this side view.

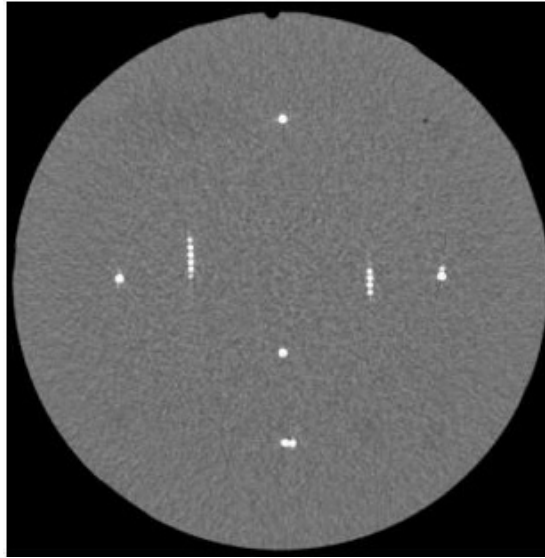


To illustrate how the bead ramps are used, the following illustration shows both a 1mm and 2mm slice going through a bead ramp. You may note that as the slice thickness increases, the peak CT value for the beads decrease. This is because as the slice thickness increases, the bead's effect on the CT number of the voxel decreases, due to volume averaging. Presuming the slice thicknesses are accurate, the peak signal over background in a 1mm slice should be double that of the peak signal over the background in the 2mm slice.

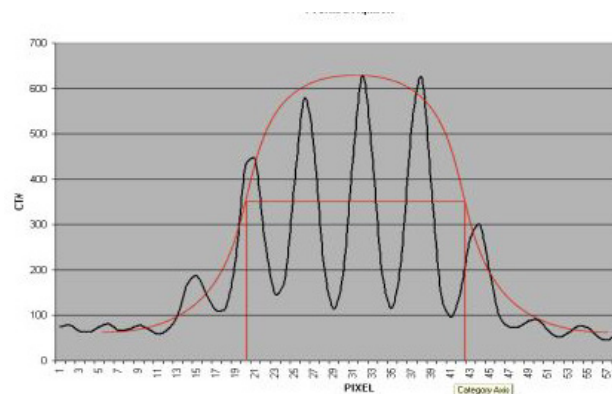


### Measuring slice thickness with a profile made from an image of the beads

Please note in this example 0.25mm spaced slice ramps are used, rather than the 1mm spaced slice ramps. The methodology for both would be basically the same, however for thinner slices the use of the fine ramps improve measurement precision. Below we use a 1mm slice scan to illustrate the use of a profile made from a line running through the bead images on the scan.



Scan of CTP591 with 1mm slice width



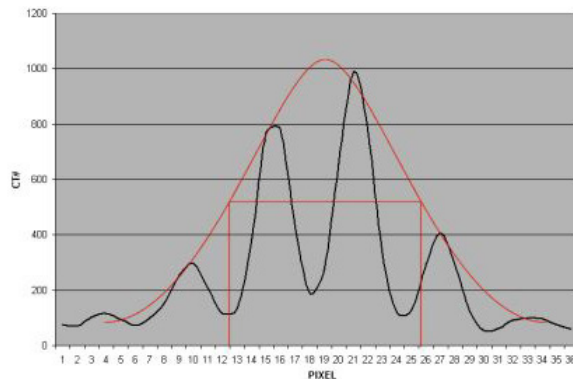
Vertical Profile of a 1mm slice through the fine .025mm bead ramps after zooming or magnification

When we use a profile line through the beads, there will be peaks at each of the bead locations and these will be separated by 0.25mm from each other. Thus for example, for the 1.0mm slice width we measure about four bead spacings at the Full Width at Half Maximum (FWHM). Multiplying the four bead spacings times the y axis increment 0.25mm per bead yields a 1mm slice width.

Another method for counting beads would be to measure the maximum CT number of the beads. This can be done by adjusting the window width to 1 and raising the level until the beads disappear and noting the peak level. Next, do an ROI of the area adjacent to the ramp to get a number for the background. Keeping the window width at 1, raise the level to half between background and peak (half maximum) and count the beads.

We can make this somewhat more analytic by noting the following. If we hand-draw, or use a mathematical “best fit” bell shaped curve (Gaussian) to the data points, you will notice that the peak CT number for the 1.0mm slice is about 650 H and the baseline is about 50, leaving a net value of about 600H between the peak value and the baseline. Thus,  $\frac{1}{2}$  the (net) maximum value is 300H + the baseline of about 50H so we draw a line across the 350H ordinate (Y) value and measure the length of the line that spans the two FWHM points at, in this case, 350H.

When measuring the FWHM of the curve it is important to realize that due to scaling and translation variables the scale of the FWHM length needs to be defined. This is done using the distance between the individual bead peaks in the profile whose absolute separation is known (.25mm for fine ramps and 1mm for coarse ramps). For example for the fine ramps divide the FWHM by the distance between bead peaks and multiply by .25mm.



Vertical Profile of a 0.5mm slice through the fine .025mm bead ramps after zooming or magnification

Please note, the typical tolerance allowed is somewhere between 0.5mm and 10% depending on the vendor.

### **Additional methods for estimating and measuring slice thicknesses with the bead ramps**

A ssp of the bead(s) can be used to measure slice thickness (see CTP528 section for additional information).

Sagittal and coronal slices through the beads can also be used to measure the axial slice width. In this case measure the z axis length at the full width at half maximum of a bead image to establish the slice thickness. However this technique is limited in precision z axis of the voxels.

The volume averaging effect on the net peak CT number of the bead can be used to approximate additional slice thickness measurements after measuring one slice's thickness by using the following equation:

w = slice width of additional slice thickness.

npvm = net peak value of the bead in the measured slice width

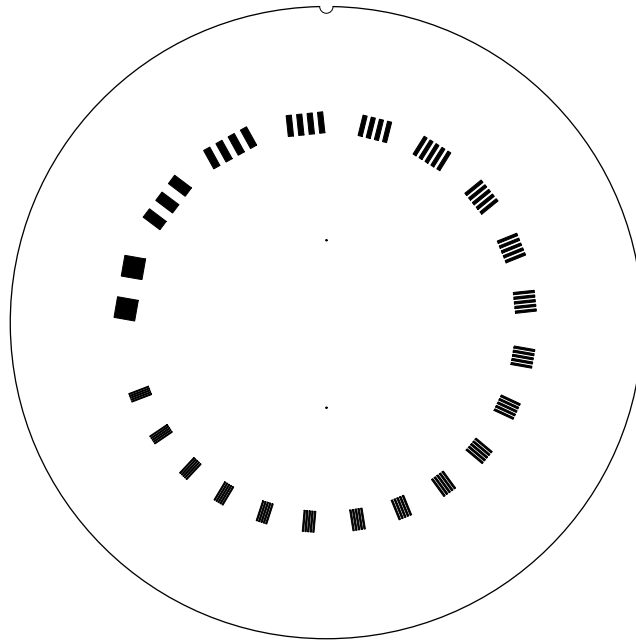
maw = slice width of the measured slice

npva = net peak value of the bead in the additional slice width

$$w = (npvm / npva) * maw$$

Note: Net peak value = (CT# of the bead) - (CT# of the background)

**CTP528 High resolution module with 21 line pair per cm gauge and point source**



This section has a 1 through 21 line pair per centimeter high resolution test gauge and two impulse sources (beads) which are cast into a uniform material. The beads are positioned along the y axis 20mm above or below the phantom's center and 2.5 and 10mm past the center of the gauge in the z direction. On older CTP528 modules the bead is aligned in the z axis with the gauge.

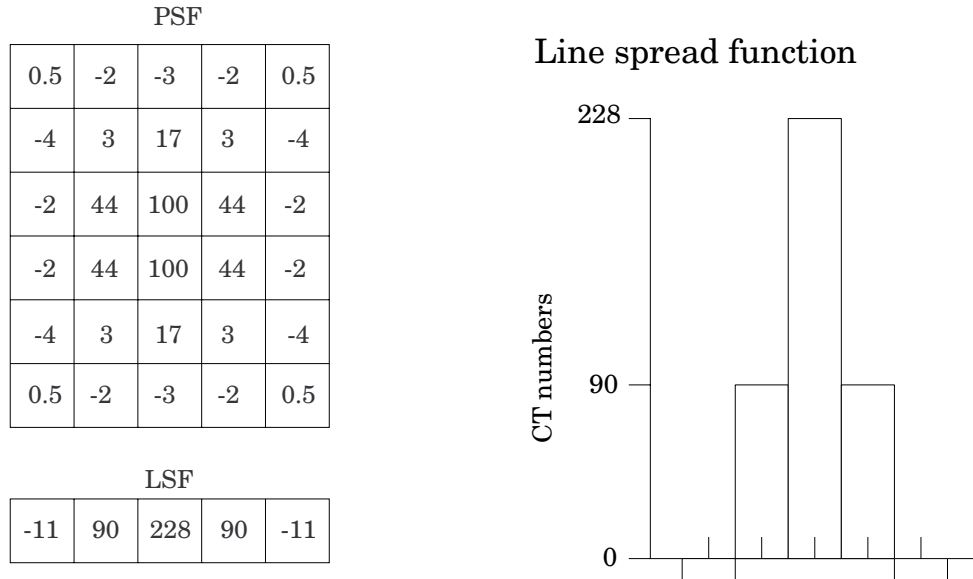
**Bead Point Source for point spread function and MTF**

Use the impulse source to estimate the point source response function of the CT system. Print out a digitized image of the area surrounding the impulse source. Use the numerical data to determine the two-dimensional array of the CT values arising from the impulse source.

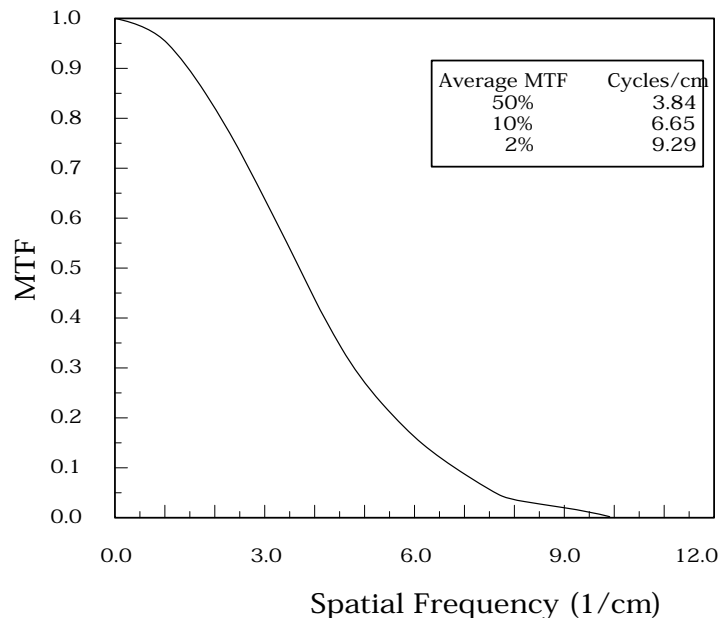
The FWHM of the point spread function is determined from the best-fit curve of the point spread function numerical data.

The average of several different arrays of impulse response functions is calculated to obtain the average point spread function of the system. These numerical values are used in conjunction with the Fourier Transform Program to provide an estimate of the two-dimensional spatial frequency response characteristics of the CT system (MTF). Illustration is on the next page.

The tungsten carbide bead has a diameter of 0.011" or 0.28mm. Because the bead is subpixel sized it is not usually necessary to compensate for it. However, some MTF programs are designed to compensate for its size.



The above illustration shows how by summing the columns (y axis) of numbers in the point spread function (PSF) the line spread function (LSF) for the x axis is obtained.



The MTF curve results from the Fourier transform of the LSF data. Generally it is easiest to use automated software for this operation. Some CT scanners are supplied with software which can calculate the MTF from the Catphan® bead images. Independent software is listed in the **Current automated programs available** section of the manual.

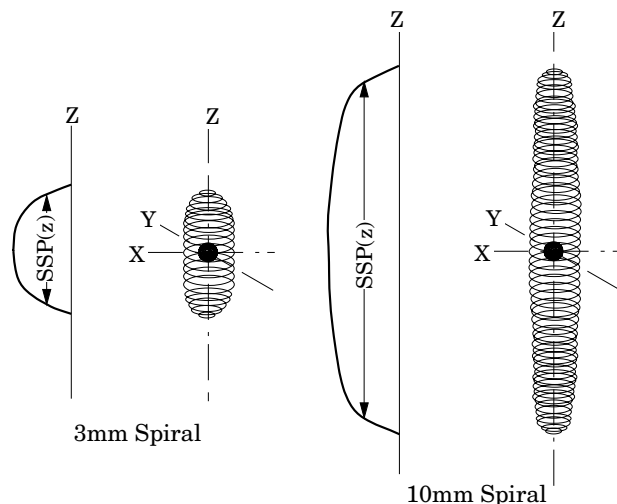
#### Use of automated scanner MTF programs

Many manufacturers include automated MTF software in the standard scanner software packages. Because the bead is cast into an epoxy background which has a different density than water, the software must accept an input for the background. The point size of .28mm must also be selected. While a sphere does produce a different density profile than a cross section of a wire or cylinder, the actual difference is not usually significant in current CT scanners.



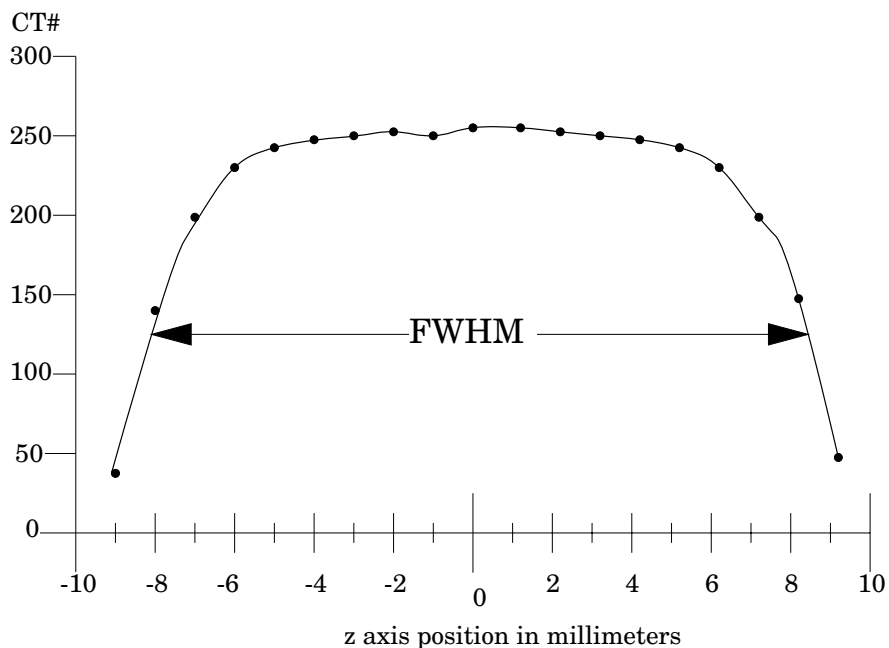
### Bead point source for slice sensitivity profile

The bead in this module can be used to calculate the slice sensitivity profile (SSP).



The above image illustrates how the bead will produce an ovoid object in a 3 dimensional reconstruction. The length of the object at the Full Width at Half Maximum signal indicates the SSP. This measurement can be easily obtained on some systems, by making a sagittal or coronal reconstruction through the bead. The bead image in these reconstructions will appear as a small line. By setting the FWHM (use the same technique described in the **Scan slice geometry** section) measuring the z axis length of the bead image to obtain the SSP.

If the scanner does not have the ability to measure z axis lengths in the sagittal or coronal planes, a SSP can be made by incrementing or spiraling the slice through the bead and reconstructing images in positive and negative table directions from the bead (using the smallest available increments) and plotting the peak CT number of the bead image in each slice. The FWHM measurement can then be made from the plotted CT values of the bead as a function of z axis table position.



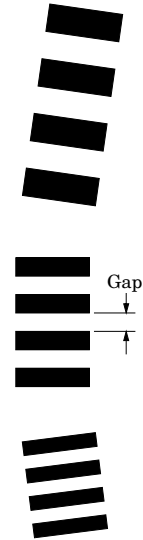
### 21 Line pair per centimeter high resolution gauge

The 21 line pair/cm gauge has resolution tests for visual evaluation of high resolution ranging from 1 through 21 line pair/cm. The gauge accuracy is  $\pm 0.5$  line pair at the 21 line pair test and even better at lower line pair tests.

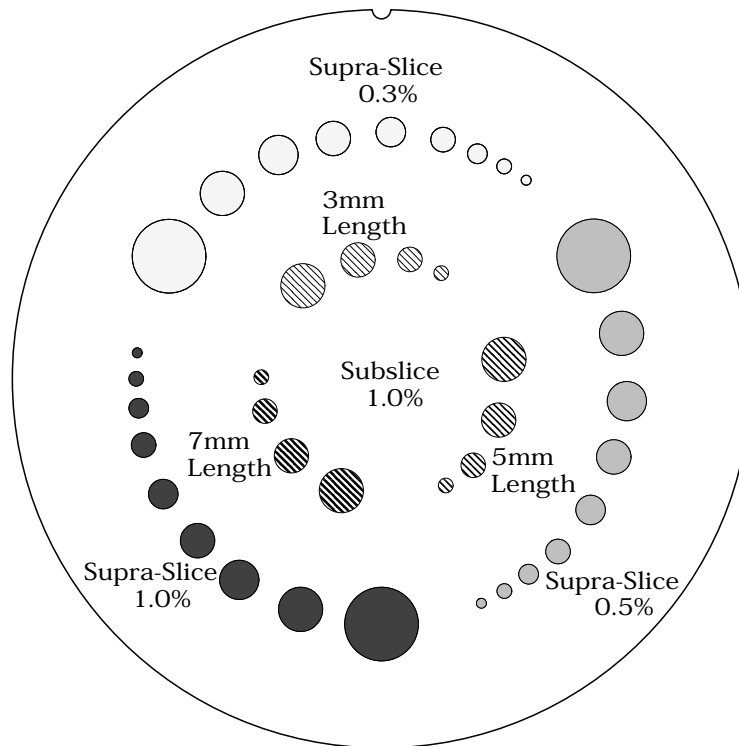
The gauge is cut from 2mm thick aluminum sheets and cast into epoxy. Depending on the choice of slice thickness, the contrast levels will vary due to volume averaging.

Line Pair/cm	Gap Size
1	0.500 cm
2	0.250 cm
3	0.167 cm
4	0.125 cm
5	0.100 cm
6	0.083 cm
7	0.071 cm
8	0.063 cm
9	0.056 cm
10	0.050 cm

Line Pair/cm	Gap Size
11	0.045 cm
12	0.042 cm
13	0.038 cm
14	0.036 cm
15	0.033 cm
16	0.031 cm
17	0.029 cm
18	0.028 cm
19	0.026 cm
20	0.025 cm
21	0.024 cm



### CTP515 low contrast module with supra-slice and subslice contrast targets



The low contrast targets have the following diameters and contrasts:

#### Supra-slice target diameters

2.0mm  
3.0mm  
4.0mm  
5.0mm  
6.0mm  
7.0mm  
8.0mm  
9.0mm  
15.0mm

#### Subslice target diameters

3.0mm  
5.0mm  
7.0mm  
9.0mm

#### Nominal target contrast levels

.3%  
.5%  
1.0%

Since the target contrasts are nominal, the actual target contrasts need to be determined before testing specific contrast performance specifications. The actual contrast levels are measured by making region of interest measurements over the larger target, and in the local background area. To determine actual contrast levels, average the measurements made from several scans. It is important to measure the background area adjacent to the measured target because “cupping” and “capping” effects cause variation of CT numbers from one scan region to another. Position the region of interest to avoid the target edges. The region of interest should be at least 4 x 4 pixels in diameter. Because low contrast measurements are “noisy” it is advisable to calculate the average of the multiple measurements made from several scans. Carefully monitor the mAs setting because the photon flux will improve with increased x-ray exposure. Use the size of the targets visualized under various noise levels to estimate information on contrast detail curves.

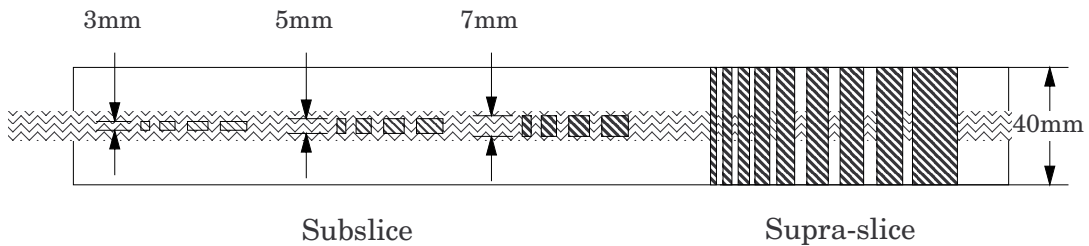
All of the targets in each contrast group are cast from a single mix to assure that the contrast levels will be the same for all targets.

The equation below can be used to convert the measured contrasts and diameters to other specified contrasts and diameters.

$$(\text{Measured Contrast}) * (\text{smallest diameter discernible}) \cong \text{Constant}$$

$$\text{example: } 5\text{mm diameter @ } 0.3\% \cong 3\text{mm diameter @ } 0.5\%$$

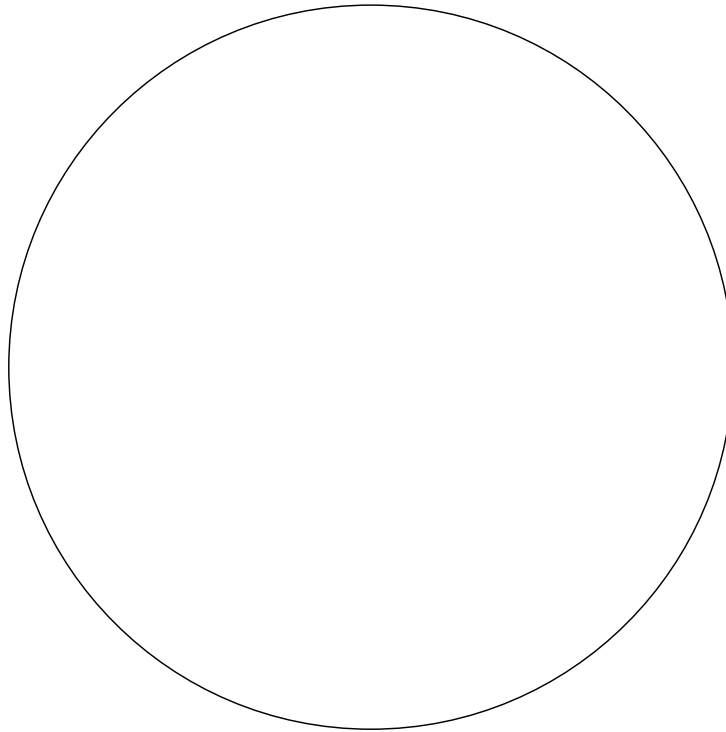
Along with the supra-slice (targets with z axis dimension longer than most maximum slice width) the CTP515 low contrast module includes subslice targets (targets with z axis length smaller than some of the usual slice width). The subslice targets are arranged in the inner circle of tests in the module.



The subslice targets are cast from the same mix as the 1.0% supra-slice targets. Because they are from the same mix in the evaluation of the actual subslice target contrast the supra-slice targets can be used to establish contrast values. The subslice targets have z axis lengths of 3, 5, and 7mm and diameters of 3, 5, 7, and 9mm.

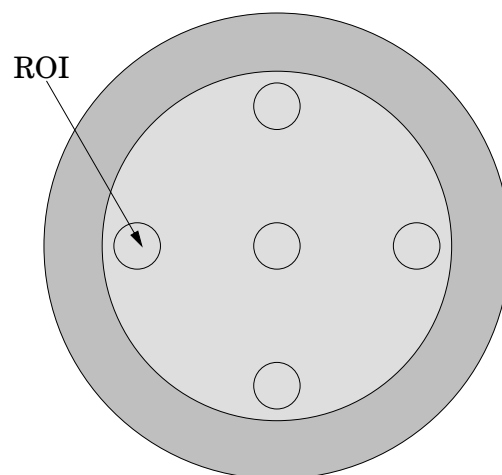
The evaluation of subslice target readability is helpful in understanding the scanner's different spiral imaging settings and how the settings will affect the ability to visualize small objects with low contrasts from their background.

### CTP486 Image uniformity module

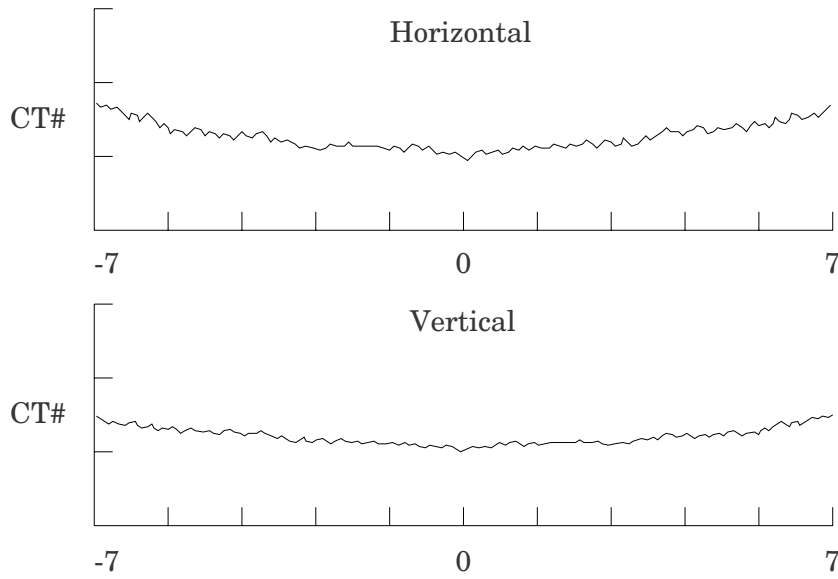


The image uniformity module is cast from a uniform material. The material's CT number is designed to be within 2% (20H) of water's density at standard scanning protocols. The typically recorded CT numbers range from 5H to 18H. This module is used for measurements of spatial uniformity, mean CT number and noise value.

The precision of a CT system is evaluated by the measurement of the mean value and the corresponding standard deviations in CT numbers within a region of interest (ROI). These measurements are taken from different locations within the scan field.



The mean CT number and standard deviation of a large number of points, (say 1000 for example) in a given ROI of the scan, is determined for central and peripheral locations within the scan image for each type of scanning protocol. Inspect the data for changes from previous scans and for correlation between neighboring slices.



Measure spatial uniformity by scanning the uniformity section. Observe the trends above and below the central mean value of a CT number profile for one or several rows or columns of pixels as shown above.

Select a profile which runs from one side of the uniformity module to the opposite side. Due to scanner boundary effects, typical profiles start 2cm from the edge of the test module.

Integral uniformity may be measured by determining the minimum and maximum CT values along the profile and by using the following equation :

$$\text{Integral Non-Uniformity} = \frac{CT_{\text{max}} - CT_{\text{min}}}{CT_{\text{max}} + CT_{\text{min}}}$$

The phenomenon of “cupping” or “capping” of the CT number may indicate the need for recalibration.

### Installation and removal of test modules

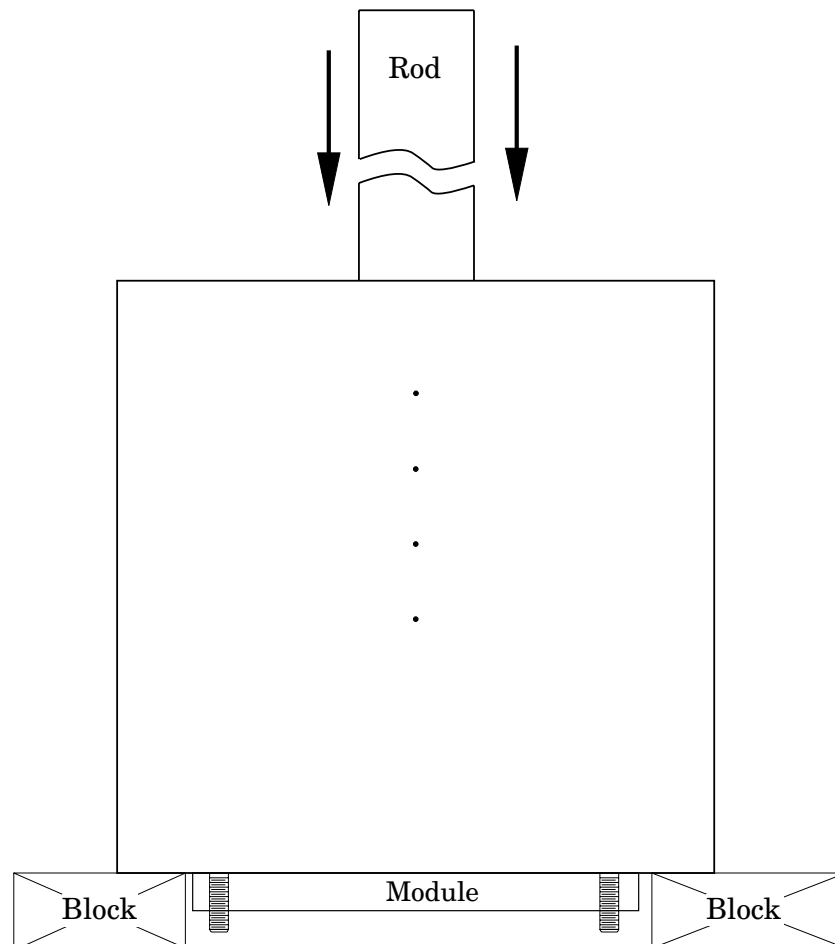
For most applications there is no need to remove modules from the Catphan®. However, modules can be removed by carefully following these steps.

Note the position of the mounting plate in relationship to the housing before removing it.

Remove the four brass nuts that secure the mounting plate to the phantom housing.

Set the phantom with the studs facing down on 2 to 4 blocks to keep the studs off the surface.

Use a blunt object, such as a wooden rod, to press the modules out of the housing.

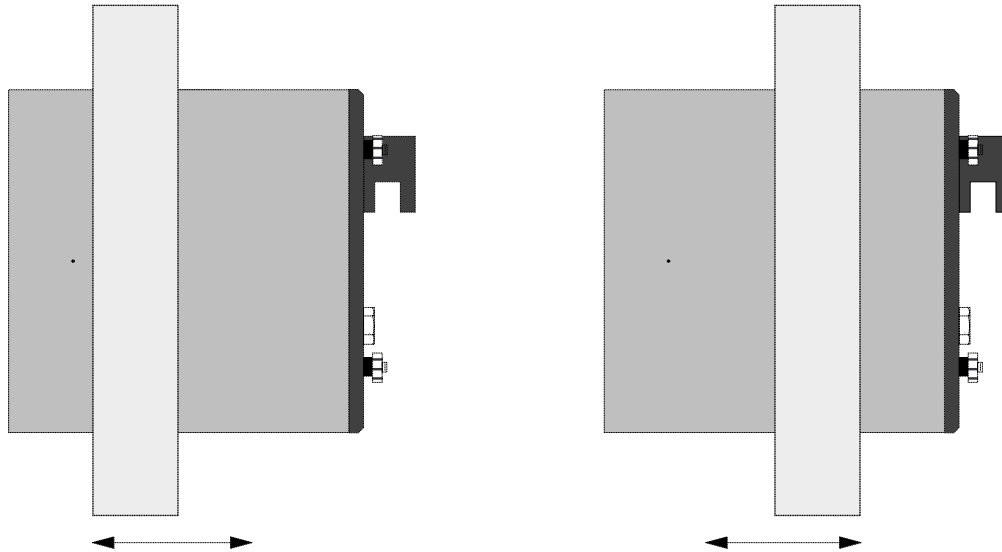


To insert modules hold the phantom housing on its side with the interior alignment key at the top. Align the module notches with the housing key as the modules are inserted one at a time into the housing. The illustrations on page 5 will indicate the correct locations of the modules.

### Optional phantom annuli

#### Warning

Before mounting a Catphan® phantom with an annulus onto the Catphan® case, the case must be secured to the table by use of the patient restraint straps or additional weight. If the case is not secured to the table when the phantom is mounted, the case, phantom and annulus could fall off the edge of the table.



The following optional annuli are designed to be used with the standard 20cm Catphan® housing.

CTP299 21.5cm diameter, Teflon annulus simulates the high absorption of bone.

CTP539 30cm diameter annulus, cast from the image uniformity material

CTP653 32cm diameter annulus, cast from the image uniformity material

CTP540 35cm diameter annulus, cast from the image uniformity material

CTP650 38cm diameter annulus, cast from the image uniformity material

CTP579 25-35cm OD oval annulus, cast from the image uniformity material

CTP651 30-38cm OD oval annulus, cast from the image uniformity material

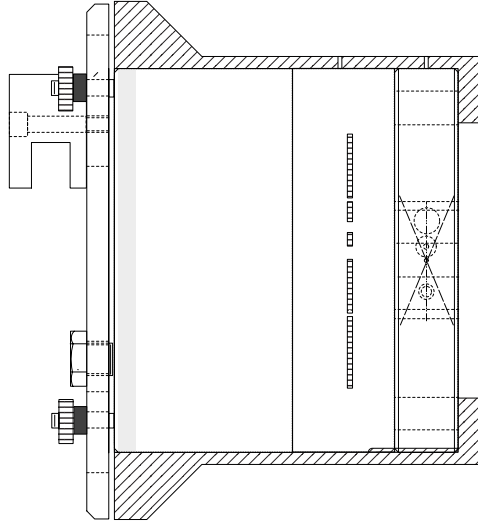
CTP599 42-55cm OD oval annulus, cast from the image uniformity material

The annuli are designed to slide over the 20cm Catphan® housing as illustrated below. Because the housing material and the uniformity annuli lack lubricity, the annuli may not slide easily. However, by adding some lubricant the resistance can be reduced.



**CTP541 16cm housing**

The CTP541 (16cm) housing will hold three Catphan® modules. Follow the instructions for removing the test modules from the 20cm housing. Insert the selected modules into the CTP541 housing.



CTP541 16cm housing shown with CTP401, CTP528 and CTP486 modules.

**Smári Analysis Service**

# Smári

For fast and accurate CT analysis, your new Catphan® purchase includes 2 years of the Smári analysis service

To register for the service, go to the Smári page at our website: [phantomlab.com](http://phantomlab.com)

You will need your phantom serial number to register, which is located on the phantom mount.



Once we receive your information, Phantom Laboratory support will contact you and set up your account.

Smári provides cloud-based automated analysis of your Catphan® phantom and tools such as longitudinal history and user specified alerts.

Test reports include:

- Spatial resolution (modulation transfer function)
- Noise and image uniformity
- Slice width and pixel size
- Sensitometry
- Contrast detectability

## Bibliography

1. AAPM Report No. 39  
Specification and Acceptance Testing of Computed Tomography Scanners  
Report of Task Group 2 Diagnostic X-Ray Imaging Committee. Published for the  
American Association of Physicists in Medicine by the American Institute of Physics.  
May 1993
  
2. M. J. Berger, J. H. Hubbell, S. M. Seltzer, J. Chang, J. S. Coarsey, R. Sukumar, and D.  
S. Zucker, Feb. 2009, XCOM: Photon Cross Sections Database, NIST Standard Reference  
Database 8 (XGAM), <http://www.nist.gov/physlab/data/xcom/index.cfm> (July 7, 2010).
  
3. Brooks and DiChiro  
Principles of Computer Assisted Tomography (CAT) in Radiographic and  
Radioisotopic Imaging  
Phys Med Biol 1976:21:689-732
  
4. Cohen and DiBanca  
The Use of Contrast-Detail-Dose Evaluation of Image Quality in a Computed  
Tomographic Scanner  
Comput. Assist. Tomogr. 3, 189-195 1979
  
5. Goodenough  
Assessment of Image Quality of Diagnostic Imaging Systems  
In: Gray GA (ed). Medical images: formation, perception and measurements. Proceedings  
of the 7th L.H.Gray Conference, New York: John Wiley & Sons, 1976:263-77
  
6. Goodenough  
Automated Quality Assurance for CT Scanners  
(Chapter): Radiology ICR 749, Editors Silver, Abecasis and Veiga-Pires. Excerpta Medica  
Press, Amsterdam 1987
  
7. Goodenough  
Psychophysical Perception of Computed Tomography Images  
In: Newton and Potts (eds). Radiology of the skull and brain: technical aspects of  
computed tomography. Vol 5, St. Louis: CV Mosby, 1981:3993-4021
  
8. Goodenough and Atkins  
Theoretical and Practical Aspects of Automated Quality Assurance Approaches,  
Particularly for CT  
Proceedings of the ICR 89, Excerpta Medica Press, Amsterdam 1990
  
9. Goodenough and Weaver  
Factors Related to Low Contrast Resolution in CT Scanners  
Computerized Radiology Vol. 8 No, 5. 279-308 1984
  
10. Goodenough, Weaver, and Davis  
Development of a Phantom for Evaluation and Assurance of Image Quality in  
CT Scanning  
The Proceedings of the Application of Optical Instrumentation in Medicine V meeting  
sponsored by The Society of Photo-Optical Instrumentation Engineers and The Society  
of Photographic Scientists and Engineers, September 16-19, 1976, Washington DC; and,  
Optical Engineering, January 1977
  
11. Goodenough, Weaver, and Davis  
Potential Artifacts Associated with the Scanning Pattern of the EMI Scanner  
Radiology 117:615-620, December 1975

12. Goodenough, Weaver, and Davis  
Physical Measurement of the EMI Imaging System  
In: Ter-Pogossian, Phelps, Brownell, Cos Jr., Davis and Evens (eds). Reconstruction tomography in diagnostic radiology and nuclear medicine. Baltimore: University Park Press, 1977: 225-243
13. John M. Boone and J. Anthony Seibert, 1997, An accurate method for computer-generating tungsten anode x-ray spectra from 30 to 140 kV, Medical Physics, v. 24, No. 11, p. 1661-1670.
14. R. J. Kriz and Keith J. Strauss, 1985, An investigation of computed tomography (CT) linearity, Medical Imaging and Instrumentation, v. 555, p. 195-204.
15. McCullough  
Photon Attenuation in Computed Tomography  
Medical Physics, 2:307-320, Nov/Dec 1975
16. McCullough, Baker, Hattery, Sheedy, Stephens and Payne  
Performance Evaluation and Quality Assurance of Computed Tomography (CT) Equipment with Illustrative Data for ACTA, Delta , and EMI Scanners  
Radiology 120: 173-188, July 1976
17. McCullough, Baker, Houser, and Reese  
An Evaluation of the Quantitative and Radiation Features of Scanning X-ray Transverse Axial Tomography: the EMI Scanner  
Radiology 111: 709-715, June 1974
18. Phelps, Hoffmar-Pogossian  
Attenuation Coefficients of Various Body Tissues, Fluids and Lesions at Photon Energies of 18 to 136 keV  
Radiology 117:573-583, December 1975
19. Rossmann  
Point Spread Function, Line Spread Function and Modulation Transfer Function: Tools for the Study of Imaging Systems  
Radiology 1969:93:257-72
20. T. R. Fewell, R. E. Shuping, and K. E. Healy, 1981, Handbook of Computed Tomography X-ray Spectra, HHS Publication (FDA) 81-8162 (U.S. Government Printing Office, Washington D.C.).
21. Weaver, Goodenough, and Briefel  
Sensitometry in Computerized Tomography  
Proceedings of SPIE, Medicine VI. 1977:127:87-94
22. Yester and Barnes  
Geometrical Limitations of Computed Tomography (CT) Scanner Resolution  
Optical instrumentation in Medicine VI. SPIE, 1977:127:296-303







